In- and Out-Degree Distributions of Nodes and Coverage in Random Sector Graphs

R. Ferrero, *Member, IEEE,* M. V. Bueno-Delgado, *Member, IEEE,* and F. Gandino, *Member, IEEE*

***Abstract*—In a random sector graph, the presence of an edge between two nodes depends on their distance and spatial orientation. This kind of graph is widely used for modeling wireless sensor networks where communication among nodes is directional. In particular, it is applied to describe both the radio frequency transmission among nodes equipped with directional antennas and the line-of-sight transmission in optical sensor networks. Important properties of a wireless sensor network, such as connectivity and coverage, can be investigated by studying the degree of the nodes of the corresponding random sector graph. In detail, the in-degree value represents the number of incoming edges, whereas the out-degree considers the outgoing edges. This paper mathematically characterizes the average degree of a random sector graph and the probability distributions of the in-degree and out-degree of the nodes. Furthermore, it derives the coverage probability of the network. All the formulas are validated through extensive simulations, showing an excellent match between theoretical results and experimental data.**

***Index Terms*—Wireless sensor network, directional antenna, optical sensor network, connectivity, topology.**

I. Introduction

A WIRELESS sensor network (WSN) consists of several electronic devices, referred to as *nodes*, that communicate through wireless transmission. Each node is equipped with a sensor to collect data from the environment, such as temperature, humidity, pressure, vibration, sound, etc. WSNs have gained great importance because of sensor nodes strengths such as low cost, low power, small size and unbounded communication. Important applications of WSNs include manufacturing process management [1], surveillance [2], precision farming [3] and healthcare [4].

A WSN is characterized by a distributed architecture: the nodes are autonomous and interact with each other to send the acquired data to a base station, by means of routing [5] or flooding [6] algorithms. Generally the wireless communication among nodes exploits radio waves, although systems that adopt free space optical transmission, such as laser light, are gathering an increasing attention.

Radio frequency transmission is a mature technology and it is currently the most widespread choice of communication for WSNs. The node is provided with a radio transceiver and an antenna. In order to increase the transmission range and to limit the energy consumption, directional antennas are usually preferred to omni-directional ones. The reduction of the interference among the nodes is another advantage of directional antennas, because the transmission areas of the nodes are narrower and less likely to overlap. The radiation model of a directional antenna consists of a high gain main lobe and some low gain sidelobes and backlobes, and it is frequently approximated to a circular sector [7], [8]. As an example, Fig. 1 shows a node i with a directional antenna: its emission signal covers a circular sector S_i, with central angle α and radius r, which corresponds to the transmission range of the antenna. The azimuth angle β indicates the antenna orientation and it is measured anticlockwise with respect to the x-axis.

WSNs where the nodes communicate through free space optical transmission are called optical sensor networks (OSNs). The nodes are equipped with a laser transmitter and with an optical device, such as a photodetector, to reflect and modulate the received light. The advantages of OSNs with respect to radio frequency WSNs include the low power consumption required by the optical transceiver, the absence of interference among the nodes and their small size due to the lightweight circuitry [9]. However the communication in an OSN requires a direct line-of-sight path between the sender and the receiver. The directed laser beam spans a circular sector of α radians and it can be randomly oriented with an angle β, as shown in Fig. 1.

Both directional radio frequency WSNs and OSNs can be represented by a family of graphs called *random sector graphs* [10], [11]. This representation is frequently used in their study and evaluation [12], [13], [14]. Each node of the network is represented by a vertex of the graph. It is assumed that the nodes are independently and uniformly deployed in a bounded region, therefore the vertices of the random sector graph are uniformly and randomly distributed. A circular sector S_i is associated to each node i: it corresponds to the area covered by the node. It is assumed that the amplitude α of the circular sector is the same for all the nodes in the graph, whereas the orientation randomly varies according to a uniform distribution. A directed edge exists from node i to j if j is located inside the sector S_i.

The edge directionality entails that a node has edges only towards its circular sector, but it can receive edges from any direction. This situation models two kinds of network. First, it is a suitable model for OSNs, because the laser transmitter of the nodes scans only a sector, but, in addition, the nodes are equipped with optical devices that passively

Manuscript received May 20, 2013; revised October 23, 2013 and January 13, 2014; accepted January 14, 2014. The associate editor coordinating the review of this letter and approving it for publication was L. Libman.

R. Ferrero and F. Gandino are with the Dipartimento di Automatica e Informatica, Politecnico di Torino, Torino, Italy (e-mail: {renato.ferrero, filippo.gandino}@polito.it).

M. V. Bueno-Delgado is with the Department of Information Technologies and Communications, Universidad Politécnica de Cartagena, Spain (e-mail: mvictoria.bueno@upct.es).

Digital Object Identifier 10.1109/TWC.2014.031314.130905

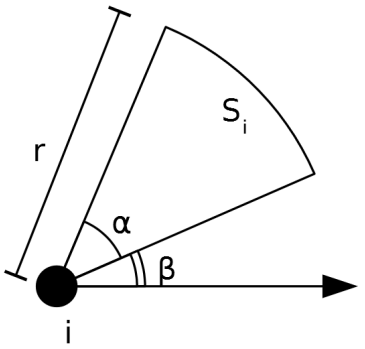

Fig. 1: Radiation model of node i.

reflect the beam received from any direction, so their sensing region is not limited to the communication sector. Secondly, it models WSNs with radio frequency transmission if the nodes have a directional transmitter antenna and an omni-directional receiver antenna.

An important topology attribute of a graph is the *degree* of its nodes. In an undirected graph, the degree d_i of node i is the number of edges that link i to other nodes. In a directed graph, a distinction is made between *in-degree* d_i^-, which is the number of edges incident to i, and *out-degree* d_i^+, which is the number of edges that depart from i.[1] The node degree is a local attribute of a graph, but its importance relies on the fact that it is directly related to global properties of the corresponding WSN, such as connectivity [15], fault tolerance [16], coverage [17] and energy consumption [18]. Therefore, the node degree directly affects the performance of the WSN and its knowledge facilitates the design and the analysis of the network.

A complete characterization of the node degree of a graph requires expressing the average degree and the degree distribution of the nodes. The average degree $E[d]$ of a graph is defined as the average number of outgoing edges that the nodes have. Since each edge links a starting node to an ending one, the average degree coincides also with the average number of incoming edges among all the nodes in the graph. The out-degree distribution $\Pr(d_i^+ = k)$ is the probability distribution of the node out-degrees over the whole graph. An analogous definition holds for the in-degree distribution $\Pr(d_i^- = k)$. Since the deployment area of a random sector graph is bounded, the average degree and the degree distribution are influenced by the *border effects* [19]: the nodes near the boundaries generally have lower degree than the other nodes, because they can be linked only to nodes toward the center.

A general description of the node degree of a random sector graph is still missing. The majority of the studies provide asymptotic results, as the number of the nodes tends to infinity [10], [20]. The Poisson distribution is adopted to approximate the degree distribution, by ignoring the border effects [21]. This paper fills the gap of the previous studies about the node degree in random sector graphs. The provided formulas of the average degree and the degree distribution consider the border effects and they are valid for any number of nodes in the graph. In addition, the theoretical analysis is validated through extensive simulations.

The remainder of this paper is organized as follows. Section II summarizes the results obtained by previous studies about the node degree in random sector graphs. Section III presents the geometrical analysis that is exploited in Sections IV and V to compute the out-degree and in-degree distributions. The expression of the average node degree is formulated in Section VI, whereas the coverage probability is deduced in Section VII. Theoretical results are validated through simulations in Section VIII. Finally, Section IX summarizes the conclusions.

II. Related Work

The asymptotic bounds of the maximum in- and out-degree among the nodes of a random sector graph deployed in the unit square $[0,1]^2$ are investigated in a couple of studies [10], [20]. The analysis in [10] exploits a dissection technique by subdividing the deployment area into a grid of s square identical cells. It is assumed that r and $\sqrt{s}$ are inversely proportional and that the sector graph contains at least $n = (1+\epsilon)s\ln s$ nodes, where ϵ is a positive constant. If the above conditions hold, an asymptotic result follows from the Chernoff and Union bounds. With probability approaching to 1 as s tends to infinity, the maximum in-degree is lower than or equal to the maximum out-degree, and their lower and upper bounds are proportional to $\ln s$ and ϵ. The same result holds for the minimum in- and out-degree.

As in [10], so the analysis in [20] imposes a relationship between transmission range and cardinality of the random sector graph. If the constraint $r \ll \sqrt{\ln n/n}$ is satisfied, a concentration result allows to almost determine the maximum in- and out-degree. The probability distribution of the maximum in- and out-degree is concentrated on two consecutive integers as n tends to infinity.

The out-degree distribution in random sector graphs is investigated in [21]. Given n nodes randomly and independently deployed in the unit square $[0,1]^2$, the number of nodes that are located in a finite subregion of area $|R|$ asymptotically converges to a Poisson distribution with mean $n|R|$, as n grows to infinity [22]. By definition, the out-degree of a node corresponds to the number of nodes located in its sensing area. Therefore, considering the planar square region $[0,1]^2$, the out-degree distribution is expressed in [21] as a Poisson distribution:

$$\Pr(d_i^+ = k)_{\text{Poisson}} = \frac{e^{\frac{-\alpha n r^2}{2}} \left(\frac{\alpha n r^2}{2}\right)^k}{k!} \,. \tag{1}$$

However, (1) does not consider the border effects. The sensing area is surely $\frac{1}{2}\alpha r^2$ only if the distance between the node and the nearest border is higher than r; otherwise, depending on the azimuth angle β, a portion of the sensing area may overstep the deployment region and the number of nodes that it contains becomes lower. The approximation introduced by (1) is acceptable only if the border effects are negligible, i.e., $r \ll 1$ in case that the deployment area is the unit square.

[1] In the paper, the notation d_i is applied also to the directed sector graph to indicate both the in-degree and out-degree, when it is assumed that their distributions coincide.

Another contribution of [21], which is also conjectured in [23], is the estimation of the probability that the in-degree of a node is zero:

$$\Pr(d_i^- = 0) = e^{\frac{-\alpha n r^2}{2}} \ . \tag{2}$$

As (1), so (2) ignores the border effects. For example, an immediate consequence of the two equations is $\Pr(d_i^+ = 0) = \Pr(d_i^- = 0)$. However, the simulations performed in [21] and in Section VIII show that, due to the border effects, the number of nodes without incident edges is always lower than or equal to the number of nodes without outgoing edges.

(1) is also obtained as a particular case of the more general analysis conducted in [24]. Here a family of sector graphs larger than the one defined in [10] is considered: the nodes are deployed according to a spatial probability distribution function $f(x)$. If $\alpha \geq \pi$, both the in- and out-degree distributions are expressed as:

$$\Pr(d_i = k) = \Pr(d_i^+ = k) = \Pr(d_i^- = k) = \\ = \frac{\left(\frac{\alpha n r^2}{2}\right)^2}{k!} \int_{\mathbb{R}^2} e^{\frac{-\alpha n r^2}{2} f(x)} f(x)^{k+1} \mathrm{d}x \ . \tag{3}$$

If the node positions follow the uniform density function $f(x) = 1_{[0,1]^2}(x)$, the degree distribution obtained after solving the integral in (3) is a Poisson distribution with mean $\frac{1}{2}\alpha t$: this result coincides with (1).

All the previous works studied only the asymptotic behavior of the node degree in random sector graphs, as the number of the nodes tends to infinity. Only marginal results about the degree distribution are provided, such as its maximum value or the probability of node isolation, otherwise the degree distribution is approximated with a Poisson distribution, by ignoring the border effects.

III. Area Covered by a Node

In a homogeneous WSN, the amplitude α of the emission beam and the transmission range r are the same for all the nodes. Ideally, all the circular sectors associated to the nodes of the corresponding random sector graph have area $\frac{\alpha r^2}{2}$ and they only differ in their azimuth angle. However, this assumption is true only if the deployment area is infinite or if a toroidal distance metric is adopted. In the latter case, each border is considered adjacent to the opposite one: the flat deployment area becomes a torus. Instead, considering a finite deployment area with an Euclidean distance metric, some circular sectors are smaller because their borders overlap.

The evaluation of the intersection between S_i and the deployment area A is generalized by considering a rectangle of length l and width w instead of the unit square as deployment area. The deployment area can be divided in four kinds of region, as shown in Fig. 2:

- an inner rectangular region A_A, whose sides have distance r from the corresponding borders of A.
- four rectangular regions A_B: two of them measure $(w - 2r) \times r$, while the other two measure $(l - 2r) \times r$.
- four regions A_C, obtained by picking the square with side r and one vertex in common with a vertex of A and by removing from it the circular sector of radius r, centered in the common vertex.
- four circular sectors A_D with radius r, whose center coincides with a vertex of A.

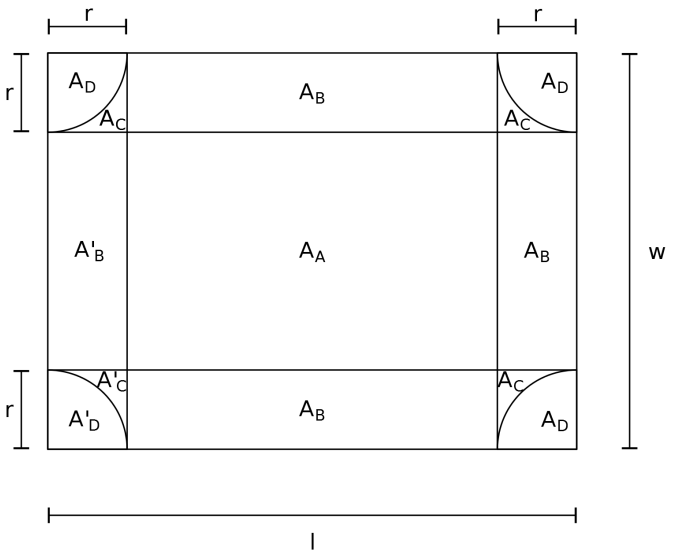

Fig. 2: Partition of the deployment area.

A is assumed large enough such that $r \leq \frac{1}{2}\min(l, w)$.

Given a node placed in point $P = (x, y) \in A$, the distances of the node from the nearest horizontal and vertical borders are denoted as:

$$d_x = \min(x, l - x) \ , \tag{4}$$

$$d_y = \min(y, w - y) \ . \tag{5}$$

Further, let d_m be the distance from the nearest border:

$$d_m = \min(d_x, d_y) \ . \tag{6}$$

The intersection area between the sector S of the node and A depends on the region where the sector is centered. A preliminary result about the intersection area is obtained by imposing the following two conditions:

1) the center P of S belongs to A_A or to one of the 3 regions marked with the prime symbol in Fig. 2.
2) the orientation angle of S is $\beta = 0$.

Let $f(\alpha, x, y, r, l, w)$ be the function that computes the intersection area in the following regions of A:

$$f(\alpha, x, y, r, l, w) = \tag{7}$$
$$\begin{cases} f_A(\alpha, r) & \text{if } (x, y) \in A_A \\ f_B(\alpha, d_x, r) & \text{if } (x, y) \in A'_B \\ f_C(\alpha, d_x, d_y, r) & \text{if } (x, y) \in A'_C \\ f_D(\alpha, d_x, d_y, r) & \text{if } (x, y) \in A'_D \ . \end{cases}$$

If the node is placed in A_A, its sector does not overlap the borders of A, therefore the intersection area is simply:

$$f_A(\alpha, r) = \frac{r^2}{2}\alpha \ . \tag{8}$$

If the sector S is centered in A'_B, it may overlap with a border, depending on the value of α. This situation is enlarged in Fig. 3. For small values of α, the sector is entirely included

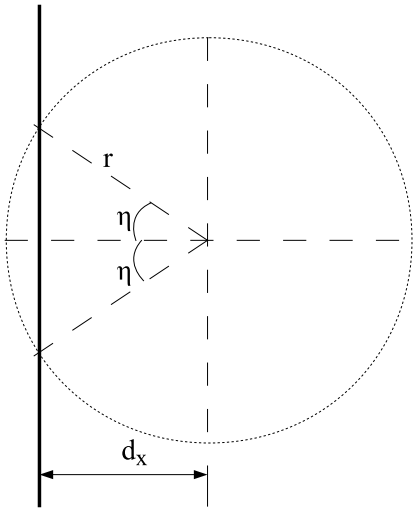

Fig. 3: Intersection between S and A'_B.

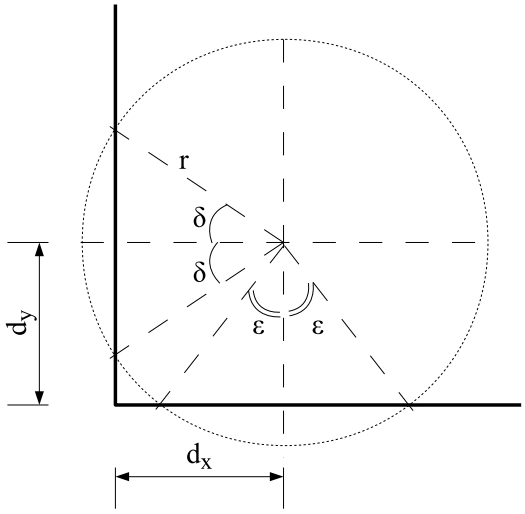

Fig. 4: Intersection between S and A'_C.

in A, but, as α increases, at a certain point it comes out from the leftmost border of A. Hence the intersection area is given by a piecewise function:

$$f_B(\alpha, d_x, r) = \tag{9}$$
$$\begin{cases} \frac{r^2}{2}\alpha & \text{if } 0 \le \alpha < \pi - \eta \\ \frac{r^2}{2}(\pi - \eta) + \frac{d_x^2}{2}(\tan\eta + \tan\alpha) & \text{if } \pi - \eta \le \alpha < \pi + \eta \\ r^2\left(\frac{\alpha}{2} - \eta\right) + d_x^2 \tan\eta & \text{if } \pi + \eta \le \alpha < 2\pi \ , \end{cases}$$

where $\eta = \arccos\left(\frac{d_x}{r}\right)$, as shown in Fig. 3. The function is defined in the domain [0, 2π[, but the domain can be extended in the following way:

$$h_B(\alpha, d_x, r) = \left\lfloor \frac{\alpha}{2\pi} \right\rfloor g_B(d_x, r) + f_B(\alpha \bmod 2\pi, d_x, r) \tag{10}$$

where

$$g_B(d_x, r) = r^2(\pi - \eta) + d_x^2 \tan\eta \ . \tag{11}$$

The intersection area between a sector S centered in A'_C and A is calculated in a similar way. Fig. 4 enlarges the bottom left corner of A; hence, the intersection is:

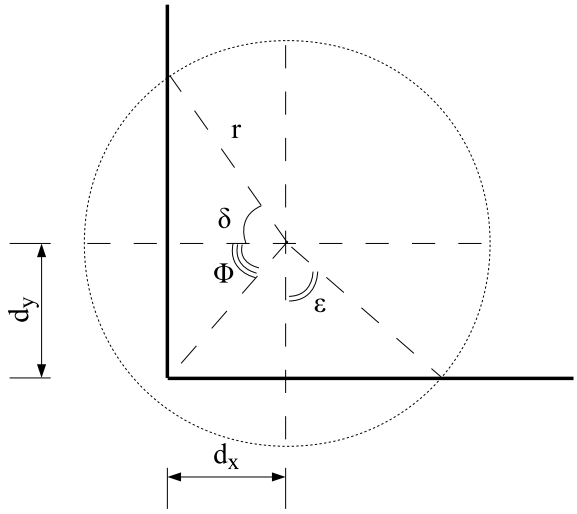

Fig. 5: Intersection between S and A'_D.

$$f_C(\alpha, d_x, d_y, r) = \tag{12}$$
$$\begin{cases} \frac{r^2}{2}\alpha & \text{if } 0 \le \alpha < \pi - \delta \\ \frac{r^2}{2}(\pi - \delta) + \frac{d_x^2}{2}(\tan\delta + \tan\alpha) & \text{if } \pi - \delta \le \alpha < \pi + \delta \\ \frac{r^2}{2}(\alpha - 2\delta) + d_x^2 \tan\delta & \text{if } \pi + \delta \le \alpha < \frac{3\pi}{2} - \epsilon \\ \frac{r^2}{2}\left(\frac{3\pi}{2} - 2\delta - \epsilon\right) + d_x^2 \tan\delta + & \\ + \frac{d_y^2}{2}\left(\tan\epsilon + \tan\left(\alpha + \frac{\pi}{2}\right)\right) & \text{if } \frac{3\pi}{2} - \epsilon \le \alpha < \frac{3\pi}{2} + \epsilon \\ r^2\left(\frac{\alpha}{2} - \delta - \epsilon\right) + d_x^2 \tan\delta + & \\ + d_y^2 \tan\epsilon & \text{if } \frac{3\pi}{2} + \epsilon \le \alpha < 2\pi \ , \end{cases}$$

where $\delta = \arccos\left(\frac{d_x}{r}\right)$ and $\epsilon = \arccos\left(\frac{d_y}{r}\right)$, as shown in Fig. 4. The following function extends the domain of (12)

$$h_C(\alpha, d_x, d_y, r) = \\ = \left\lfloor \frac{\alpha}{2\pi} \right\rfloor g_C(d_x, d_y, r) + f_C(\alpha \bmod 2\pi, d_x, d_y, r) \ , \tag{13}$$

where

$$g_C(d_x, d_y, r) = r^2(\pi - \delta - \epsilon) + d_x^2 \tan\delta + d_y^2 \tan\epsilon \ . \tag{14}$$

Fig. 5 enlarges the bottom left corner of A when the sector S is centered within A'_D. The intersection area between S and A is given by the following function:

$$f_D(\alpha, d_x, d_y, r) = \tag{15}$$
$$\begin{cases} \frac{r^2}{2}\alpha & \text{if } 0 \le \alpha < \pi - \delta \\ \frac{r^2}{2}(\pi - \delta) + \frac{d_x^2}{2}(\tan\delta + \tan\alpha) & \text{if } \pi - \delta \le \alpha < \pi + \phi \\ \frac{r^2}{2}(\pi - \delta) + \frac{d_x^2}{2}\tan\delta + & \\ + \frac{d_y^2}{2}\tan\left(\alpha + \frac{\pi}{2}\right) + d_x d_y & \text{if } \pi + \phi \le \alpha < \frac{3\pi}{2} + \epsilon \\ \frac{r^2}{2}\left(\alpha - \frac{\pi}{2} - \delta - \epsilon\right) + & \\ + \frac{d_x^2}{2}\tan\delta + \frac{d_y^2}{2}\tan\epsilon + d_x d_y & \text{if } \frac{3\pi}{2} + \epsilon \le \alpha < 2\pi \ , \end{cases}$$

where $\phi = \arctan\left(\frac{d_y}{d_x}\right)$, as shown in Fig. 5. The domain is [0, 2π[, but it is extended by the following function:

$$h_D(\alpha, d_x, d_y, r) = \tag{16}$$
$$= \left\lfloor \frac{\alpha}{2\pi} \right\rfloor g_D(d_x, d_y, r) + f_D(\alpha \bmod 2\pi, d_x, d_y, r) \ ,$$

where

$$g_D(d_x, d_y, r) = \tag{17}$$
$$= \frac{r^2}{2}\left(\frac{3\pi}{2} - \delta - \epsilon\right) + \frac{d_x^2}{2}\tan\delta + \frac{d_y^2}{2}\tan\epsilon + d_x d_y \ .$$

By generalizing to a sector S with center $P \in A$ and any orientation angle β, its intersection area with A is:

$$f_{S\cap A}(\alpha, \beta, x, y, r, l, w) = \tag{18}$$
$$\begin{cases} f_A(\alpha, r) & \text{if } (x,y) \in A_A \\ h_B(\alpha+\beta, d_m, r) - f_B(\beta, d_m, r) & \text{if } (x,y) \in A_B \\ h_C(\alpha+\beta, d_x, d_y, r) - f_C(\beta, d_x, d_y, r) & \text{if } (x,y) \in A_C \\ h_D(\alpha+\beta, d_x, d_y, r) - f_D(\beta, d_x, d_y, r) & \text{if } (x,y) \in A_D \ . \end{cases}$$

By defining the following function:

$$h(\alpha, x, y, r, l, w) = \tag{19}$$
$$\begin{cases} f_A(\alpha, r) & \text{if } (x,y) \in A_A \\ h_B(\alpha, d_m, r) & \text{if } (x,y) \in A_B \\ h_C(\alpha, d_x, d_y, r) & \text{if } (x,y) \in A_C \\ h_D(\alpha, d_x, d_y, r) & \text{if } (x,y) \in A_D \ , \end{cases}$$

the area of the intersection between a circular sector and the deployment area can be written in short as:

$$f_{S\cap A}(\alpha, \beta, x, y, r, l, w) =$$
$$= h(\alpha+\beta, x, y, r, l, w) - f(\beta, x, y, r, l, w) \ . \tag{20}$$

IV. Out-degree Distribution

In a random sector graph, the out-degree of a node is given by the number of other nodes inside its circular sector. The probability that a node is within a circular sector is directly proportional to the area of the sector. The reason lies in the fact that, since the nodes are randomly deployed according to a uniform distribution, each point of the deployment area A has the same probability of containing a node. Thus, the probability that a node located at $P \in A$ is placed in a subarea R is:

$$\Pr(P \in R) = \frac{|R \cap A|}{|A|} \ . \tag{21}$$

Ignoring the border effects, the out-degree of a node, i.e., the probability that k nodes fall in its circular sector and the others are outside, is a binomial distribution:

$$\Pr(d^+ = k)_{\text{binom}} = \binom{n-1}{k}\left(\frac{\alpha r^2}{2lw}\right)^k\left(1 - \frac{\alpha r^2}{2lw}\right)^{n-k-1} . \tag{22}$$

Due to the border effects, the area of the circular sector S_i of a generic node i is obtained by integrating (20) with respect to l, w, β and then by dividing the result by the ranges of integration. Then, the probability p that a direct edge exists from i to another node j is obtained by dividing this resulting area by $|A|$. The presence of an edge between nodes i and j can be regarded as a Bernoulli trial with probability of success p. The estimation of the number of edges that depart from node i corresponds to the repetition of $n-1$ independent Bernoulli trials, each one with success probability p. Hence, the out-degree distribution is given by:

$$\Pr(d^+ = k) =$$
$$= \binom{n-1}{k}\frac{1}{2\pi|A|}\int_0^w\int_0^l\int_0^{2\pi}\left(\frac{f_{S\cap A}(\alpha,\beta,x,y,r,l,w)}{|A|}\right)^k$$
$$\cdot\left(1 - \frac{f_{S\cap A}(\alpha,\beta,x,y,r,l,w)}{|A|}\right)^{n-k-1} \mathrm{d}\beta\,\mathrm{d}y\,\mathrm{d}x \ . \tag{23}$$

Due to the additivity of integration on intervals, the integral in (23) can be partially solved by splitting it in each of the four subdomains of $f_{S\cap A}(\alpha, \beta, x, y, r, l, w)$. For the region A_A, the integral is directly solved. In the other regions, the integrals are simplified by means of a change of variables: the new variables of integration are the distances d_x and d_y from the borders. In particular, this substitution simplifies the triple integral on the region A_B to a double one. The formula for the out-degree distribution becomes:

$$\Pr(d^+ = k) =$$
$$= \binom{n-1}{k}\frac{1}{2\pi|A|}\left(2\pi|A_A|\left(\frac{\alpha r^2}{2|A|}\right)^k\left(1 - \frac{\alpha r^2}{2|A|}\right)^{n-k-1} + \right.$$
$$+ \frac{|A_B|}{r}\int_0^r\int_0^{2\pi}\left(\frac{h_B(\alpha+\beta,d_m,r) - f_B(\beta,d_m,r)}{|A|}\right)^k\cdot$$
$$\cdot\left(1 - \frac{h_B(\alpha+\beta,d_m,r) - f_B(\beta,d_m,r)}{|A|}\right)^{n-k-1} \mathrm{d}\beta\,\mathrm{d}d_m +$$
$$+ 4\int_0^r\int_{\sqrt{r^2-d_x^2}}^r\int_0^{2\pi}$$
$$\left(\frac{h_C(\alpha+\beta,d_x,d_y,r) - f_C(\beta,d_x,d_y,r)}{|A|}\right)^k\cdot$$
$$\cdot\left(1 - \frac{h_C(\alpha+\beta,d_x,d_y,r) - f_C(\beta,d_x,d_y,r)}{|A|}\right)^{n-k-1}$$
$$\mathrm{d}\beta\,\mathrm{d}d_y\,\mathrm{d}d_x + 4\int_0^r\int_0^{\sqrt{r^2-d_x^2}}\int_0^{2\pi}$$
$$\left(\frac{h_D(\alpha+\beta,d_x,d_y,r) - f_D(\beta,d_x,d_y,r)}{|A|}\right)^k\cdot$$
$$\cdot\left(1 - \frac{h_D(\alpha+\beta,d_x,d_y,r) - f_D(\beta,d_x,d_y,r)}{|A|}\right)^{n-k-1}$$
$$\left.\mathrm{d}\beta\,\mathrm{d}d_y\,\mathrm{d}d_x\right) \ . \tag{24}$$

V. In-degree Distribution

The in-degree of node i counts the number of edges from other nodes to i. There is a directed edge towards i if the following two conditions hold. First, all the edges incident to i depart from nodes whose distance from i is lower than or equal to r. Let Q be the set of points in A whose distance from i is lower than or equal to r. According to (21), the probability that j is placed within a distance r from i is given by the ratio between the areas of Q and A. The second necessary condition is the inclusion of i in the circular sector covered by j: the probability of success of this event is $\alpha/2\pi$. By combining

the two conditions, it follows:

$$\Pr(i \in S_j) = \frac{\alpha}{2\pi}\frac{|Q|}{|A|} \ . \tag{25}$$

If the border effects are ignored, (25) is easily evaluated: in this case, Q becomes a circle of area πr^2. Therefore, the in-degree distribution coincides with the out-degree distribution:

$$\Pr(d^- = k)_{\text{binom}} = \Pr(d^+ = k)_{\text{binom}} = \Pr(d = k)_{\text{binom}} \ . \tag{26}$$

However, due to the presence of the border effects, Q corresponds to a circle only if the distance of i from the borders of the deployment area A is higher than r, otherwise its area is lower because it partially overlaps A. The intersection area between a circle and the deployment area is provided in [25]:

$$g_{C\cap A}(x,y,r,l,w) = \tag{27}$$
$$\begin{cases} \pi r^2 & \text{if } (x,y) \in A_A \\ g_B(d_m, r) & \text{if } (x,y) \in A_B \\ g_C(d_x, d_y, r) & \text{if } (x,y) \in A_C \\ g_D(d_x, d_y, r) & \text{if } (x,y) \in A_D \ . \end{cases}$$

It follows that the in-degree probability distribution is given by:

$$\begin{aligned} &\Pr(d^- = k) = \\ &= \binom{n-1}{k}\frac{1}{|A|}\int_0^w\int_0^l \left(\frac{\alpha}{2\pi}\frac{g_{C\cap A}(x,y,r,l,w)}{|A|}\right)^k \cdot \\ &\cdot \left(1 - \frac{\alpha}{2\pi}\frac{g_{C\cap A}(x,y,r,l,w)}{|A|}\right)^{n-k-1} \mathrm{d}y\,\mathrm{d}x \ . \end{aligned} \tag{28}$$

An alternative formula of the in-degree probability distribution is provided by splitting the integral of (28) in the four subdomains:

$$\begin{aligned} &\Pr(d^- = k) = \\ &= \binom{n-1}{k}\frac{1}{|A|}\left(|A_A|\left(\frac{\alpha r^2}{2|A|}\right)^k\left(1-\frac{\alpha r^2}{2|A|}\right)^{n-k-1} + \frac{|A_B|}{r}\cdot\right. \\ &\cdot \int_0^r \left(\frac{\alpha}{2\pi}\frac{g_B(d_m,r)}{|A|}\right)^k\left(1-\frac{\alpha}{2\pi}\frac{g_B(d_m,r)}{|A|}\right)^{n-k-1}\mathrm{d}d_m + \\ &+ 4\int_0^r\int_{\sqrt{r^2-d_x^2}}^r \left(\frac{\alpha}{2\pi}\frac{g_C(d_x,d_y,r)}{|A|}\right)^k \cdot \\ &\cdot \left(1-\frac{\alpha}{2\pi}\frac{g_C(d_x,d_y,r)}{|A|}\right)^{n-k-1}\mathrm{d}d_y\,\mathrm{d}d_x + \\ &+ 4\int_0^r\int_0^{\sqrt{r^2-d_x^2}} \left(\frac{\alpha}{2\pi}\frac{g_D(d_x,d_y,r)}{|A|}\right)^k \cdot \\ &\left.\cdot \left(1-\frac{\alpha}{2\pi}\frac{g_D(d_x,d_y,r)}{|A|}\right)^{n-k-1}\mathrm{d}d_y\,\mathrm{d}d_x\right) \ . \end{aligned} \tag{29}$$

VI. Average Degree

Let X be a discrete random variable that takes values $x_0, x_1, \ldots$, with probability $p_0, p_1, \ldots$, respectively. The expected value of X is given by:

$$E[X] = \sum_{k=0}^{\infty} x_k p_k \ . \tag{30}$$

Thus the average value of the out-degree distribution is:

$$E[d^+] = \sum_{k=0}^{n-1} k \cdot \Pr(d^+ = k) \ . \tag{31}$$

By substituting the formula of the degree distribution provided in (23), it follows:

$$\begin{aligned} E[d^+] &= \sum_{k=0}^{n-1}\left(k\cdot\binom{n-1}{k}\frac{1}{2\pi|A|}\cdot\right. \\ &\cdot \int_0^w\int_0^l\int_0^{2\pi}\left(\frac{f_{S\cap A}(\alpha,\beta,x,y,r,l,w)}{|A|}\right)^k \cdot \\ &\left.\cdot\left(1-\frac{f_{S\cap A}(\alpha,\beta,x,y,r,l,w)}{|A|}\right)^{n-k-1}\mathrm{d}\beta\,\mathrm{d}y\,\mathrm{d}x\right) \ . \end{aligned} \tag{32}$$

The linearity property of the integral states that the integral of a linear combination is the linear combination of the integrals, therefore:

$$\begin{aligned} E[d^+] &= \frac{1}{2\pi|A|}\int_0^w\int_0^l\int_0^{2\pi}\sum_{k=0}^{n-1}\left(k\binom{n-1}{k}\cdot\right. \\ &\cdot\left(\frac{f_{S\cap A}(\alpha,\beta,x,y,r,l,w)}{|A|}\right)^k \cdot \\ &\left.\cdot\left(1-\frac{f_{S\cap A}(\alpha,\beta,x,y,r,l,w)}{|A|}\right)^{n-k-1}\mathrm{d}\beta\,\mathrm{d}y\,\mathrm{d}x\right) \ . \end{aligned} \tag{33}$$

The function to be integrated is the summation of k multiplied by a binomial distribution with success probability $p = f_{S\cap A}(\alpha,\beta,x,y,r,l,w)/|A|$. According to (30), the result of the summation is the expected value of the distribution: since the average value of the binomial distribution is given by the number of trials multiplied by the success probability, it follows:

$$\begin{aligned} E[d^+] &= \frac{1}{2\pi|A|}\cdot \\ &\cdot \int_0^w\int_0^l\int_0^{2\pi}(n-1)\left(\frac{f_{S\cap A}(\alpha,\beta,x,y,r,l,w)}{|A|}\right)\mathrm{d}\beta\,\mathrm{d}y\,\mathrm{d}x \ . \end{aligned} \tag{34}$$

The following lemma is used to reduce the triple integral to a double one.

Lemma 1. *Average coverage area.* Given a deployment surface A of length l and width w, let S be a sector centered at point $P = (x,y) \in A$, with radius r, amplitude α and azimuth β. The average area covered by S is proportional only to α and $g_{C\cap A}(\alpha,x,y,r,l,w)$.

Proof: in each of the regions identified in Fig. 2, the average value of the coverage area is provided by integrating (20) with respect to α from 0 to 2π and then by dividing it by the range of integration:

$$\begin{aligned} m(\alpha,x,y,r,l,w) &= \frac{1}{2\pi}\int_0^{2\pi} f_{S\cap A}(\alpha,\beta,x,y,r,l,w)\mathrm{d}\beta = \\ &= \frac{1}{2\pi}\int_0^{2\pi} h(\alpha+\beta,x,y,r,l,w)\mathrm{d}\beta + \\ &- \frac{1}{2\pi}\int_0^{2\pi} f(\beta,x,y,r,l,w)\mathrm{d}\beta \ . \end{aligned} \tag{35}$$

With the substitution $\gamma = \alpha + \beta$, the integral becomes:

$$\begin{aligned} m(\alpha,x,y,r,l,w) &= \frac{1}{2\pi}\int_{\alpha}^{2\pi+\alpha} h(\gamma,x,y,r,l,w)\mathrm{d}\gamma + \\ &- \frac{1}{2\pi}\int_{0}^{2\pi} f(\beta,x,y,r,l,w)\mathrm{d}\beta = \\ &= \frac{1}{2\pi}\int_{\alpha}^{2\pi+\alpha} \left\lfloor \frac{\gamma}{2\pi} \right\rfloor g_{C\cap A}(x,y,r,l,w)\mathrm{d}\gamma + \\ &+ \frac{1}{2\pi}\int_{\alpha}^{2\pi+\alpha} f(\gamma \bmod 2\pi,x,y,r,l,w)\mathrm{d}\gamma + \\ &- \frac{1}{2\pi}\int_{0}^{2\pi} f(\beta,x,y,r,l,w)\mathrm{d}\beta \ . \end{aligned} \tag{36}$$

Since $0 \le \alpha < 2\pi$ and $0 \le \beta < 2\pi$, then $0 \le \gamma < 4\pi$:

$$\begin{aligned} m(\alpha,x,y,r,l,w) &= \frac{1}{2\pi}\int_{2\pi}^{2\pi+\alpha} g_{C\cap A}(x,y,r,l,w)\mathrm{d}\gamma + \\ &+ \frac{1}{2\pi}\Bigg(\int_{\alpha}^{2\pi} f(\gamma,x,y,r,l,w)\mathrm{d}\gamma + \\ &+ \int_{0}^{\alpha} f(\gamma,x,y,r,l,w)\mathrm{d}\gamma - \int_{0}^{2\pi} f(\beta,x,y,r,l,w)\mathrm{d}\beta \Bigg). \end{aligned} \tag{37}$$

The sum inside the brackets is zero, therefore it is proved

$$m(\alpha,x,y,r,l,w) = \frac{\alpha}{2\pi} g_{C\cap A}(x,y,r,l,w) \ . \tag{38}$$

because $g_{C\cap A}(x,y,r,l,w)$ is not function of γ. ■

By applying lemma 1, (35) becomes:

$$E[d^+] = \frac{\alpha(n-1)}{2\pi|A|}\int_0^w\int_0^l \frac{g_{C\cap A}(x,y,r,l,w)}{|A|}\mathrm{d}y\,\mathrm{d}x \ . \tag{39}$$

The integral is solved by splitting it in the four subdomains of $g_{C\cap A}(x,y,r,l,w)$:

$$\begin{aligned} E[d^+] &= \frac{\alpha(n-1)}{2\pi|A|^2}\Bigg((w-2r)(l-2r)\pi r^2 + \frac{\pi^2+1}{2}r^4 + \\ &+ (w+l-4r)\left(2\pi - \frac{4}{3}\right)r^3 + \left(4\pi - \frac{1}{2}\pi^2 - \frac{16}{3}\right)r^4\Bigg) = \\ &= (n-1)\frac{\alpha}{2\pi}\left(\frac{r}{wl}\right)^2\left(\frac{1}{2}r^2 - \frac{4}{3}(w+l)r + \pi wl\right) \ . \end{aligned} \tag{40}$$

The same result is obtained if the average value of the in-degree distribution is computed:

$$E[d^-] = \sum_{k=0}^{n-1} k \cdot \Pr(d^- = k) \ . \tag{41}$$

Following the same steps, (41) leads to the calculus of the double integral of $g_{C\cap A}(x,y,r,l,w)$, with respect to w and l. Therefore, it is proved:

$$E[d] = E[d^+] = E[d^-] \ . \tag{42}$$

VII. Coverage

An important global property of a WSN is the coverage, which evaluates how well the WSN monitors the region A of interest. More formally, a point $P \in A$ is covered if it falls in the sensing area of at least one node of the WSN. The concept of coverage can be extended in the following way: given a positive integer k, P is k-covered if it is located within the sensing areas of at least k nodes. The k-coverage probability is the probability that a point inside the deployment area is covered by at least k nodes.

According to (25), the probability that a fixed point P is not covered by any sensor is:

$$\Pr(P \text{ is not covered}) = \left(1 - \frac{\alpha}{2\pi}\frac{|Q|}{|A|}\right)^n \ , \tag{43}$$

where Q is the set of points whose distance from P is lower than or equal to r. If the border effects are ignored, $|Q| = \pi r^2$ and the probability that P is covered easily follows:

$$\begin{aligned} \Pr(\text{coverage})_{\text{no border}} &= \Pr(P \text{ is covered})_{\text{no border}} = \\ &= 1 - \left(1 - \frac{\alpha r}{2lw}\right)^n \ . \end{aligned} \tag{44}$$

The coverage probability is given by (44) because, without border effects, every point has the same probability of being covered by at least one sensor.

Due to the border effects, the probability that P is covered depends on its coordinate (x_p, y_p):

$$\Pr(P \text{ is covered}) = 1 - \left(1 - \frac{\alpha}{2\pi}\frac{g_{C\cap A}(x_p,y_p,r,l,w)}{lw}\right)^n \ . \tag{45}$$

The coverage probability is obtained by integrating (45) over A:

$$\begin{aligned} &\Pr(\text{coverage}) = \\ &= 1 - \frac{1}{|A|}\int_0^w\int_0^l \left(1 - \frac{\alpha}{2\pi}\frac{g_{C\cap A}(x_p,y_p,r,l,w)}{lw}\right)^n \mathrm{d}y\,\mathrm{d}x \ . \end{aligned} \tag{46}$$

The k-coverage probability is determined similarly. The probability that less than k sensors cover P is:

$$\begin{aligned} &\Pr(P \text{ is not } k\text{-covered}) = \\ &= \sum_{i=0}^{k-1}\binom{n}{i}\left(\frac{\alpha}{2\pi}\frac{|Q|}{|A|}\right)^i\left(1 - \frac{\alpha}{2\pi}\frac{|Q|}{|A|}\right)^{n-i} \ . \end{aligned} \tag{47}$$

The k-coverage probability in a WSN with n nodes can be obtained by the in-degree distribution in a random sector graph with $n+1$ nodes. For example, by ignoring the border effects, the k-coverage probability is:

$$\begin{aligned} &\Pr(k\text{-coverage with } n \text{ nodes})_{\text{binom}} = \\ &= 1 - \sum_{i=0}^{k-1}\Pr(d = i \text{ with } n+1 \text{ nodes})_{\text{binom}} \ . \end{aligned} \tag{48}$$

If the summation of the binomial distributions is approximated with a summation of Poisson distributions, (48) becomes:

$$\begin{aligned} &\Pr(k\text{-coverage with } n \text{ nodes})_{\text{Poisson}} = \\ &= 1 - \sum_{i=0}^{k-1}\Pr(d = i \text{ with } n \text{ nodes})_{\text{Poisson}} \ . \end{aligned} \tag{49}$$

The formulation of the k-coverage probability that considers the presence of the border effects is:

$$\begin{aligned} &\Pr(k\text{-coverage with } n \text{ nodes}) = \\ &= 1 - \sum_{i=0}^{k-1}\Pr(d^- = i \text{ with } n+1 \text{ nodes}) \ . \end{aligned} \tag{50}$$

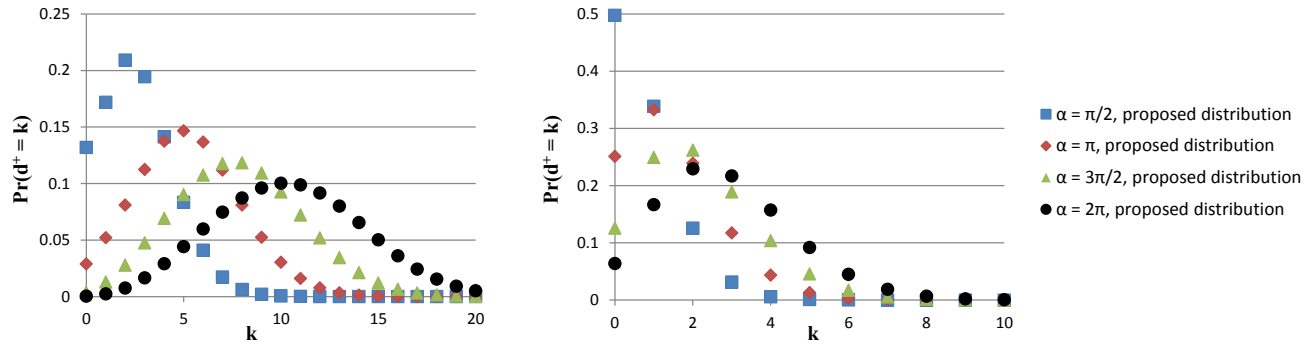

(a) $5r \times 5r$ deployment area. (b) $10r \times 10r$ deployment area.

Fig. 6: Out-degree distribution.

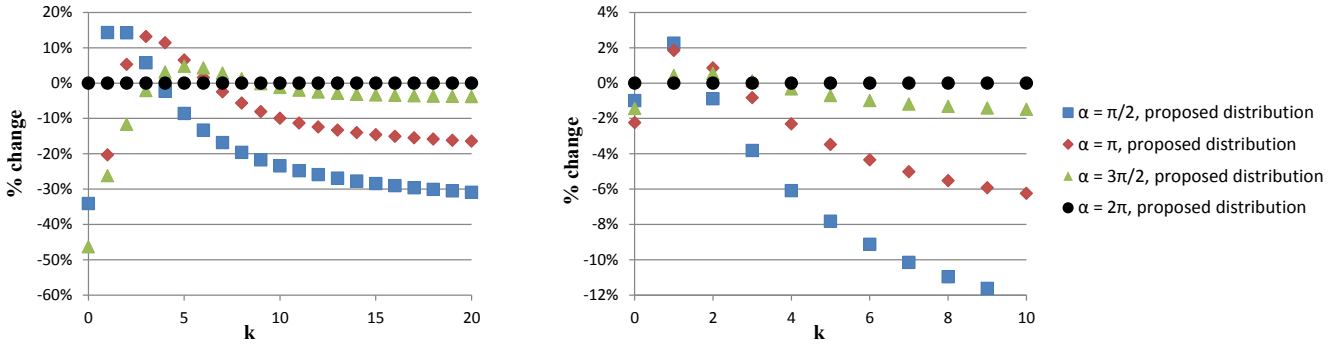

(a) $5r \times 5r$ deployment area. (b) $10r \times 10r$ deployment area.

Fig. 7: Percentage change of the in-degree distribution with respect to the out-degree distribution.

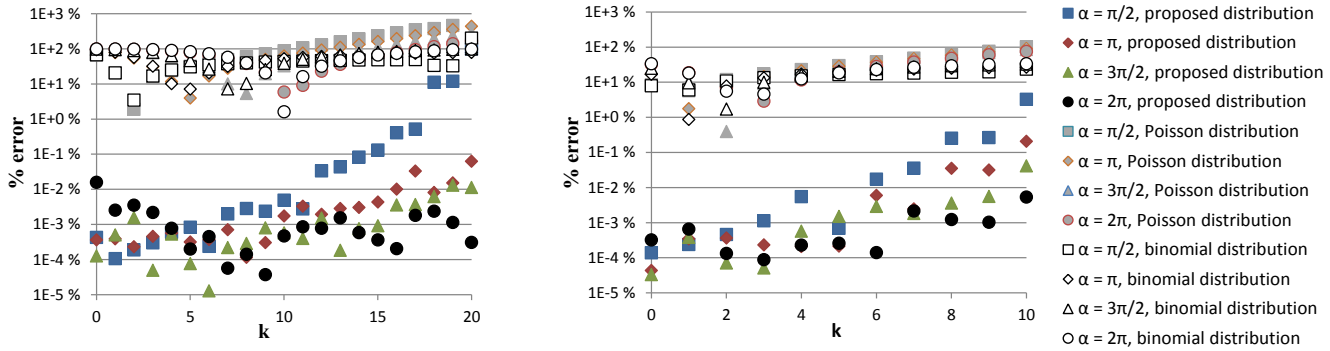

(a) $5r \times 5r$ deployment area. (b) $10r \times 10r$ deployment area.

Fig. 8: Percentage error of the out-degree distribution with respect to simulations.

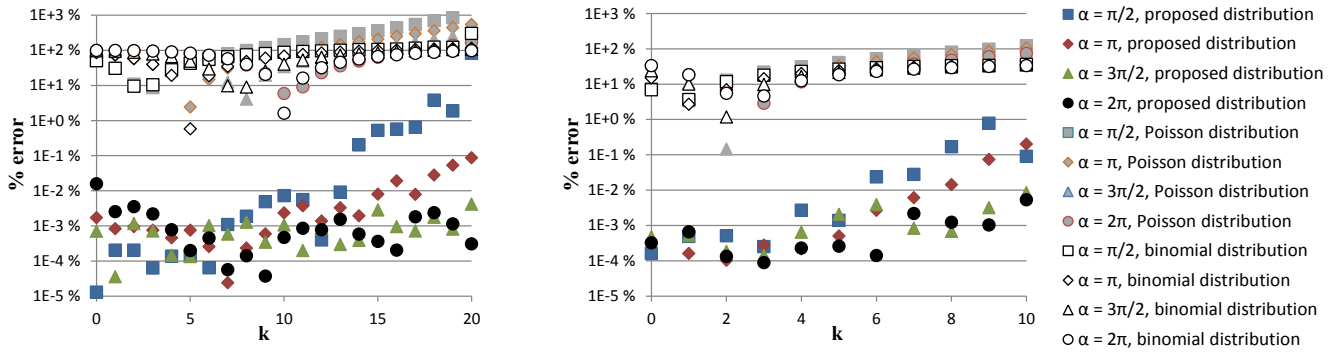

(a) $5r \times 5r$ deployment area. (b) $10r \times 10r$ deployment area.

Fig. 9: Percentage error of the in-degree distribution with respect to simulations.

VIII. Evaluation and Validation

Different scenarios are considered for evaluating the in- and out-degree distributions of nodes in a random sector graph. $n = 100$ nodes are deployed in a square region of variable side w, proportional to the transmission radius: $w \in [5r, 10r]$. For each deployment area, different random sector graphs are built by varying the amplitude of the circular sector associated to the nodes: $\alpha \in [\pi/2, 2\pi]$. If $\alpha = 2\pi$, the random sector graph becomes a random geometric graph [26]: this graph is undirected and the only condition for the presence of an edge between two nodes is that their distance should be lower than r. Analytic results of the in- and out-degree distributions are obtained by numerically integrating (24) and (29) through the *Mathematica* tool[2]. The scripts used for the computations are publicly available[3].

As depicted in Fig. 6, the provided out-degree distribution resembles the Poisson distribution. The probability that a node has out-degree $k > 0$ tend to decrease as the size of the deployment area increases. At the same time, the lower α is, the fewer edges the node has.

The trend of the in-degree distribution is similar to the one of the out-degree distribution. In order to highlight their differences, Fig. 7 shows the percentage change of the in-degree distribution with respect to the out-degree distribution, calculated as follows:

$$\%\ \text{change} = \frac{\Pr(d^- = k) - \Pr(d^+ = k)}{\Pr(d^+ = k)} \cdot 100\ . \qquad (51)$$

The probability that no edge enters into a node is always lower than or equal to the probability that the node has no outgoing edges, as already noticed in [21]. However, the curve of the in-degree distribution immediately and dramatically rises. In particular, the *mode*, i.e., the most frequent value, is the same for the in- and out-degree distributions, but it holds:

$$\Pr(d^- = mode) \geq \Pr(d^+ = mode)\ . \qquad (52)$$

In the right half, the in-degree distribution reduces more sharply than the out-degree distribution. Its percentage change with respect to the out-degree distribution is more accentuated if the deployment area is small: as the side of A increases, the difference between the two distributions levels off at some percentage points. Furthermore, the in-degree distribution approaches the out-degree distribution as the value of α increases. The reason is that, given a node i, the probability that the circular sector associated to i contains all the nodes with edges incident to i is directly proportional to the amplitude of the circular sector. As a case limit, if $\alpha = 2\pi$, the two distributions match, because the graph becomes an undirected random geometric graph.

The accuracy of the proposed in- and out-degree distributions was measured through simulations. A simple Java program was developed to automatically build random sector graphs. The implemented algorithm randomly deploys 100 nodes according to a uniform distribution and then it collects statistics about the number of incoming and outgoing edges for each node. The Java program was executed on an Intel Core i7-2600 octa-core processor, with 7.8 GB of RAM and clock speed of 3.40 GHz. The time required for the generation of one sector graph and its degree calculation is on the order of 1 ms and it depends on the size of A and α. In order to reduce the effect of randomness, statistical results are averaged among 10^9 repetitions for each configuration previously described. The difference between the proposed distribution and the data extrapolated from the simulations is expressed through the percentage error, calculated as:

$$\%\ \text{error} = \frac{|\text{value}_{\text{theoretical}} - \text{value}_{\text{simulation}}|}{\text{value}_{\text{simulation}}} \cdot 100\ . \qquad (53)$$

Fig. 8 reports, on a logarithmic scale, the percentage error of the proposed out-degree distribution. In order to provide a basis for comparison, the figure displays in light gray the percentage error of the Poisson distribution, which is suggested as an approximation of the out-degree distribution in [21], [24]. With respect to (1), the mean of the Poisson distribution is $\frac{\alpha n r^2}{2|A|}$, since the deployment area is not unitary. Furthermore, Fig. 8 also shows the percentage error of the binomial distribution given by (22): the corresponding markers are white with a black outline. The percentage error between the proposed out-degree distribution and the simulation data is generally comprised between 0.0001% and 0.1%. The slight difference is due to the approximation of the numerical integration of (24) and to the randomness in the simulations. On the contrary, the Poisson and the binomial distributions noticeably diverge from the simulations because they do not consider the border effects. The approximation introduced by the Poisson distribution with respect to the binomial distribution is marginal compared to the error due to the border effects, therefore the two distributions show a similar trend. Independently of the distribution, the percentage error tends to rise as the node degree increases, because the values obtained from the simulations are smaller and even a minimal discrepancy with the theoretical values produces a high percentage difference.

Similarly to the out-degree distribution, Fig. 9 shows an excellent match between the proposed in-degree distribution and the data observed from simulations, with a very low percentage error. The Poisson and binomial distributions for the in-degree are the same of the out-degree, as confirmed by (3) and (26). By comparing Fig. 8 and 9, it can be noted that the patterns are essentially the same, with an increase of the percentage error for all the distributions in correspondence to higher node degree due to the small absolute value of the reference data.

Given a node, (23) states that each edge towards another node has the same probability of existing, independently of other edges. However, this identical edge probability does not contradict the fact that edge occurrences are correlated. For example, if an edge from node i to j exists, this implies a higher probability for an edge from j to i than if there would be no edge from i to j. In order to show that the edge dependencies do not impact on the equiprobability of edge existence, the similarity between the experimental data and the theoretical out-degree distribution has been computed for each simulation. If the probabilities of having an edge to any of the other nodes were independent only in different realizations of

[2]http://www.wolfram.com/mathematica

[3]http://ubi.polito.it/research/randomSectorGraph.htm

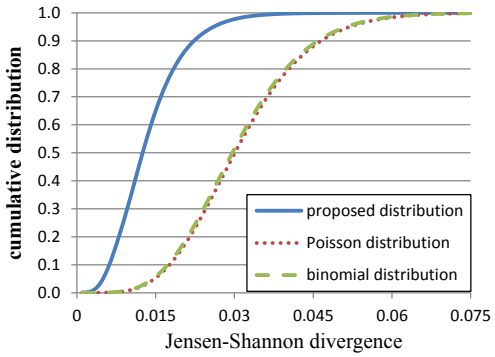

Fig. 10: Jensen-Shannon divergence of out-degree distribution in a $5r \times 5r$ deployment area with $\alpha = \pi/2$.

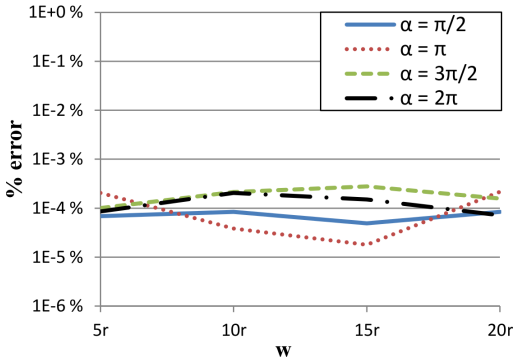

Fig. 12: Percentage error of the average node degree with respect to simulations.

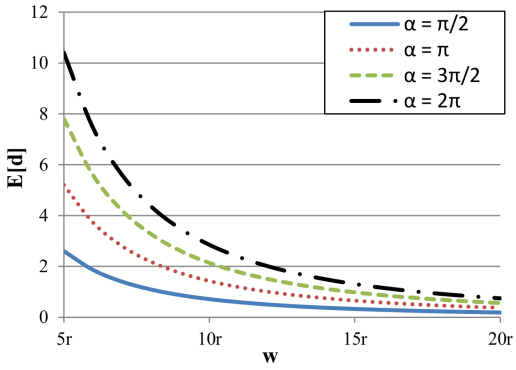

Fig. 11: Average node degree.

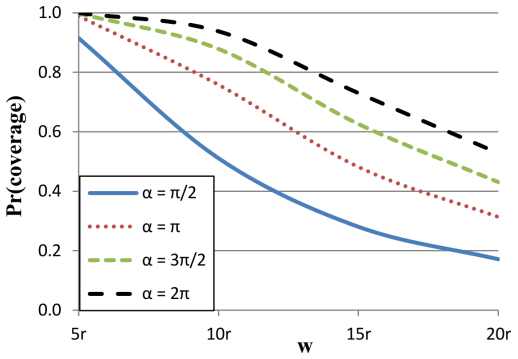

Fig. 13: Coverage probability.

the network, then each simulation would notably diverge from the theoretical distribution. Instead, Fig. 10 reveals that the divergence is lower than 0.03 in almost all the simulations. The divergence was measured by means of the Jensen-Shannon divergence [27], whose upper bound is $\ln(2)$. Given two discrete probability distributions P and Q, it is defined as:

$$D_{SD}(P \parallel Q) = \frac{1}{2} D_{KL}(P \parallel M) + \frac{1}{2} D_{\mathrm{KL}}(Q \parallel M) \ , \quad (54)$$

where $M = \frac{1}{2}(P + Q)$ and D_{KL} is the Kullback-Leibler divergence, defined as follows:

$$D_{KL}(P \parallel Q) = \sum_i \ln\left(\frac{P(i)}{Q(i)}\right) P(i) \ . \quad (55)$$

It is worth noting that the Poisson and binomial approximations of the out-degree distribution distance more from each simulations: the divergence threshold that includes almost all the cases is the double than the one required by the proposed distribution.

Fig. 11 plots the theoretical average degree of a random sector graph, by varying the deployment area and the amplitude of the circular sector in the evaluation of (40). A linear relationship holds between the average node degree and α: for example, the average degree of a random sector graph with $\alpha = \pi$ is the half of the one of a random geometric graph. Further, the average degree decays as the side w of the deployment area increases, because the nodes become less densely deployed. The exactness of (40) is confirmed by its negligible percentage error displayed in Fig. 12. The agreement of the simulation results with the theoretical curve is perfect: the observed gap is only due to the randomness in the simulations, because (40) is a closed-form expression and no approximation is made in its computation.

Finally, Fig. 13 depicts the theoretical coverage probability expressed by (50), for different values of deployment and sensing areas. The conditions for an almost complete coverage are a small deployment area, with side up to 5 times the transmission radius of the nodes, and antennas with amplitude higher than $\pi/2$. If the deployment area enlarges, the lower is the antenna amplitude, the faster the coverage probability decreases. Since (50) takes into account the border effects for evaluating the coverage probability, it is extremely accurate, as proved in Fig. 14. On the contrary, (48) and (49) reveal an exceptionally higher percentage error. This trend is expected, because the network coverage is directly related to the in-degree distribution, therefore the error introduced by the Poisson and binomial approximations of the degree distribution has significant repercussion on the coverage probability.

IX. Conclusion

The present paper has analyzed the node degree in random sector graphs. Previous results in this field overlooked the bounded area where the nodes of the graph are deployed and only asymptotic analyses were performed, as the size of the deployment area and the number of the nodes tend to infinity. In particular, the out-degree distribution was fit to a Poisson distribution, by ignoring the border effects that reduce the coverage area of the nodes. No formulation was proposed for the average node degree. This paper has bridged the gap by

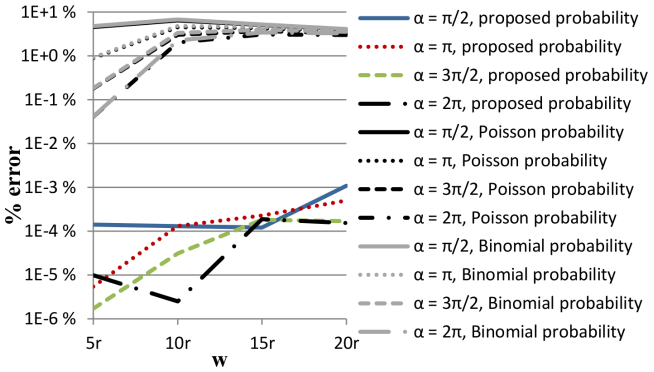

Fig. 14: Percentage error of the coverage probability with respect to simulations.

providing precise expressions for in- and out-degree distributions, average degree and coverage probability. The proposed out-degree distribution has been evaluated through numerical integration and has been compared with data obtained from extensive simulations. The percentage error almost entirely ranges between 0.0001% and 0.1%: a higher percentage error happens only for the values at the right extremity of the distribution, which are characterized by very few occurrences. Instead, it has been shown that the Poisson distribution poorly matches the out-degree distribution of a random sector graph because its percentage error with respect to the experimental data is comprised between 10% and 100%. The accuracy of the proposed distribution for the node in-degree is almost the same as the one of the out-degree distribution. The percentage error made in the evaluation of the average node degree is even lower, because a closed-form expression is provided and its difference from experimental data is only due to randomness in the simulations. The same accuracy characterizes the formula of the coverage probability.

ACKNOWLEDGMENT

This work has been partially funded by the MINECO/FEDER project grant CALM TEC2010-21405-C02-02, research project UPCT-3639/13TIC and also developed within the framework of "Programa de Ayudas a Grupos de Excelencia de la Region deMurcia", funded by Fundacion Seneca, Agencia de Ciencia y Tecnologia de la Region de Murcia (Plan Regional de Ciencia y Tecnologia 2007/2010).

REFERENCES

[1] M. Akhondi, A. Talevski, S. Carlsen, and S. Petersen, "Applications of wireless sensor networks in the oil, gas and resources industries," in *Proc. 2010 IEEE International Conf. Advanced Inf. Netw. Applications*, pp. 941–948.

[2] K. Ren, K. Zeng, and W. Lou, "Secure and fault-tolerant event boundary detection in wireless sensor networks," *IEEE Trans. Wireless Commun.*, vol. 7, no. 1, pp. 354–363, 2008.

[3] D. Chaudhary, S. Nayse, and L. Waghmare, "Application of wireless sensor networks for greenhouse parameter control in precision agriculture," *International J. Wireless Mobile Netw.*, vol. 3, no. 1, pp. 140–149, 2011.

[4] J. Ko, C. Lu, M. Srivastava, J. Stankovic, A. Terzis, and M. Welsh, "Wireless sensor networks for healthcare," *Proc. IEEE*, vol. 98, no. 11, pp. 1947–1960, 2010.

[5] A. Abdulla, H. Nishiyama, J. Yang, N. Ansari, and N. Kato, "HYMN: a novel hybrid multi-hop routing algorithm to improve the longevity of WSNs," *IEEE Trans. Wireless Commun.*, vol. 11, no. 7, pp. 2531–2541, 2012.

[6] L. Zhang, R. Ferrero, E. R. Sanchez, and M. Rebaudengo, "Performance analysis of reliable flooding in duty-cycle wireless sensor networks," *Trans. Emerging Telecommun. Technol.*, in press.

[7] S. Yi, Y. Pei, and S. Kalyanaraman, "On the capacity improvement of ad hoc wireless networks using directional antennas," in *Proc. 2003 ACM International Symp. Mobile Ad Hoc Netw. Comput.*, ser. MobiHoc '03, pp. 108–116.

[8] H.-N. Dai, K.-W. Ng, R.-W. Wong, and M.-Y. Wu, "On the capacity of multi-channel wireless networks using directional antennas," in *Proc. 2008 IEEE Conf. Comput. Commun.*, pp. 628–636.

[9] J. M. Kahn, R. H. Katz, and K. S. J. Pister, "Next century challenges: mobile networking for 'smart dust'," in *Proc. 1999 ACM/IEEE International Conf. Mobile Comput. Netw.*, ser. MobiCom '99. ACM, pp. 271–278.

[10] J. Díaz, J. Petit, and M. Serna, "A random graph model for optical networks of sensors," *IEEE Trans. Mobile Comput.*, vol. 2, no. 3, pp. 186–196, 2003.

[11] C. Àlvarez, J. Díaz, J. Petit, J. Rolim, and M. Serna, "Efficient and reliable high level communication in randomly deployed wireless sensor networks," in *Proc. 2004 International Workshop Mobility Management Wireless Access Protocols*, ser. MobiWac '04. ACM, pp. 106–110.

[12] J. Díaz, J. Petit, and M. Serna, "Evaluation of basic protocols for optical smart dust networks," in *Experimental and Efficient Algorithms*, ser. Lecture Notes in Computer Science. Springer, 2003, vol. 2647, pp. 97–106.

[13] D. Kundur, U. N. Okorafor, and W. Luh, "HoLiSTiC: heterogeneous lightweight sensornets for trusted visual computing," in *Proc. 2006 International Conf. Intelligent Inf. Hiding Multimedia Signal Process.*, pp. 267–270.

[14] R. Xie, L.-M. Peng, W. Tang, F. Tong, D.-K. Kang, W.-H. Yang, and Y.-C. Kim, "A simulation study of neighborhood discovery algorithm in free space optical sensor networks," in *Proc. 2010 International Conf. Ubiquitous Future Netw.*, pp. 87–91.

[15] M. D. Penrose, "On k-connectivity for a geometric random graph," *Random Structures Algorithms*, vol. 15, no. 2, pp. 145–164, 1999.

[16] X.-Y. Li, P.-J. Wan, Y. Wang, and C.-W. Yi, "Fault tolerant deployment and topology control in wireless networks," in *Proc. 2003 ACM International Symp. Mobile Ad Hoc Netw. Comput.*, ser. MobiHoc '03. ACM, pp. 117–128.

[17] L.-H. Yen and C. W. Yu, "Link probability, network coverage, and related properties of wireless ad hoc networks," in *Proc. 2004 IEEE International Conf. Mobile Ad-hoc Sensor Syst.*, pp. 525–527.

[18] W. R. Heinzelman, J. Kulik, and H. Balakrishnan, "Adaptive protocols for information dissemination in wireless sensor networks," in *Proc. 1999 ACM/IEEE International Conf. Mobile Comput. Netw.*, ser. MobiCom '99. ACM, pp. 174–185.

[19] D. A. Griffith and C. G. Amrhein, "An evaluation of correction techniques for boundary effects in spatial statistical analysis: traditional methods," *Geographical Analysis*, vol. 15, no. 4, pp. 352–360, Oct. 1983.

[20] Y. Shang, "Focusing of maximum vertex degrees in random faulty scaled sector graphs," *Paramerican Mathematical J.*, vol. 22, no. 2, pp. 1–17, 2012, arXiv:0909.2933v2.

[21] U. Okorafor and D. Kundur, "On the connectivity of hierarchical directional optical sensor networks," in *Proc. 2007 IEEE Wireless Commun. Netw. Conf.*, pp. 3524–3528.

[22] N. A. Cressie, *Statistics for Spatial Data*. John Wiley & Sons, 1993.

[23] U. Okorafor and D. Kundur, "On the relevance of node isolation to the k-connectivity of wireless optical sensor networks," *IEEE Trans. Mobile Comput.*, vol. 8, no. 10, pp. 1427–1440, Oct. 2009.

[24] Y. Shang, "On the degree sequence of random geometric digraphs," *Applied Mathematical Sciences*, vol. 4, no. 41, pp. 2001–2012, 2010.

[25] R. Ferrero and F. Gandino, "Degree distribution of unit disk graphs with uniformly deployed nodes on a rectangular surface," in *Proc. 2011 International Conf. Broadband Wireless Comput., Commun. Applications*, pp. 255–262.

[26] J. Dall and M. Christensen, "Random geometric graphs," *Physical Rev. E*, vol. 66, no. 1, p. 016121, July 2002.

[27] J. Lin, "Divergence measures based on the shannon entropy," *IEEE Trans. Inf. Theory*, vol. 37, no. 1, pp. 145–151, 1991.

Renato Ferrero received the M.S. degree in computer engineering in 2004 and the Ph.D. degree in Computer Engineering in 2012, both from Politecnico di Torino, Italy. He is currently a research fellow at the Dipartimento di Automatica e Informatica of Politecnico di Torino. His research interests include ubiquitous computing, wireless sensor networks and RFID systems.

M. Victoria Bueno-Delgado received her M.Sc. degree and Ph.D in Telecommunications Engineering in 2004 and 2010 respectively, both from Universidad Politecnica de Cartagena (UPCT), Spain. In 2004 she joined at UPCT as researcher in Information Technologies and Communications Department and in 2006 she joined as Assistant professor in the same University. Her research interests include anti-collision protocols and deployment techniques in RFID systems, WSN and optical switching.

Filippo Gandino obtained his M.S. in 2005 and Ph.D. degree in Computer Engineering in 2010, from the Politecnico di Torino. He is currently an Assistant Professor with the Dipartimento di Automatica e Informatica, Politecnico di Torino. His research interests include ubiquitous computing, RFID, WSNs, security and privacy, network modeling and digital arithmetic.